6th International Conference on
Protection of Structures against Hazards
16-17 October 2014, Tianjin, China

PROTECTIVE STEEL STRUCTURES AGAINST WOODEN DEBRIS HAZARDS

Nobutaka Ishikawa*, Hajime Shibuya† , Satoshi Katsuki† and Takahisa Mizuyama‡

*Professor Emeritus of National Defense Academy, Japan
(Research Association for Steel Sabo Structures, Japan)

e-mail: <cgishikawa@m4.dion.ne.jp> webpage: http://www.koseisabo.gr.jp/

Keywords: wooden debris, trap performance, slit dam, a new DEM, cylindrical stick element

Abstract. *This paper presents a fundamental new approach at looking at protective structures (slit dams) against wooden debris hazards. First, a model test was performed to examine the trap performance of slit dams against wooden debris. Herein, the relationship between the length of wooden debris and the gap between slit dams was investigated on trap performance. Second, a new DEM (Distinct Element Method) was developed to simulate the trap performance of wooden debris with or without roots by using the three dimensional (3D) analysis introducing cylindrical stick elements. Finally, a new DEM was applied to simulate the actual wooden debris disaster site in Hiroshima, Japan.*

1 INTRODUCTION

In recent years, many natural disasters have occurred in various places of the world, including typhoons, tsunamis, floods, snow storms, avalanches, landslides, debris flows, earthquakes and volcanic eruptions. Such natural catastrophes can cause human injuries, loss of life, economic devastation, and the destruction of construction works as well as cultural and natural heritage sites. Debris flow hazards have increased through local downpours of rain, because of the seasonal rainfall or typhoon [1,2]. In particular, wooden debris hazards [3,4] have eroded the upper streams of many banks, which have led to an increase of removal costs of wooden debris in the dam reservoirs and general damage to the dam site. The blockage generated from the bridge has exacerbated the damage dealt to houses and to people's well-being, as shown in Figs.1 and 2.

.

Figure1: Blockage generated from the bridge

Figure 2: Damage dealt to houses

† Department of Civil and Environmental Engineering, National Defence Academy,Japan
‡ Graduate School of Agriculture, Kyoto University, Japan

Wooden debris is caused by the outflow of standing trees, fallen trees, cut trees as well as debris from houses and bridges [3].

To defend against the wooden debris hazards, steel slit dams [5,6,7] as shown in Figs.3 and 4, have been advocated to be built in up stream areas. The current design code [8] of steel slit dams stipulates that the ratio between the gap width (W) and the maximum length (l_{max}) of wooden debris should be less than 1/2 as shown in Fig.4. Many studies [9,10,11] have been devoted to wooden debris flow and the countermeasures against them. However, the effects of the average length of wooden debris, the gaps of slit dams, flow volume and the roots of wooden debris have not been investigated yet on the trap performance. Furthemore, a computational method with wooden debris has not yet been developed for the slit dams trap performance.

Figure 3:Trap performance against wooden debris

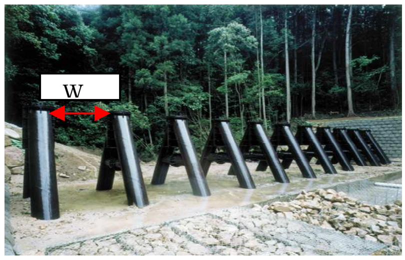

Figure 4: Gap width (W) of a slit dam

This paper presents a basic approach on trap performance of wooden debris from both an experimental and comupational points of views. First, a trap performance test was performed for wooden debris by changing the length of wooden debris and the gap width of the slit dams [12,13,14] . Second, a new DEM was developed for the trap performance of wooden debris by introducing cylidrical stick elements [15,16] into the usual DEM [17] . Finally, the new developed DEM was applied to the trap simulation of an actual disaster site of wooden debris in Hiroshima, Japan [18].

2 MODEL TEST FOR TRAP PERFORMANCE

2.1 Outline of the model test

The model test was performed by using the channel with a length of 4m, a width of 0.3m and a height of 0.5m which can change the slope of 0°~20° as shown in Fig.5. The water was supplied by a line pump and cistern. The wooden debris was dropped by using the conveyer belt.

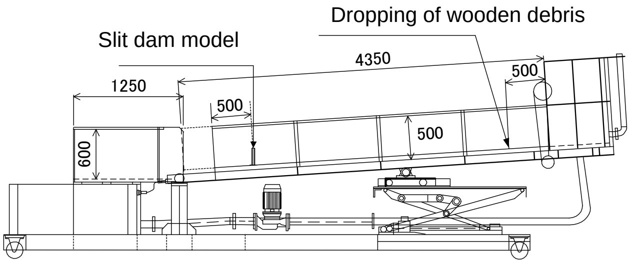

Figure 5: Model test set-up

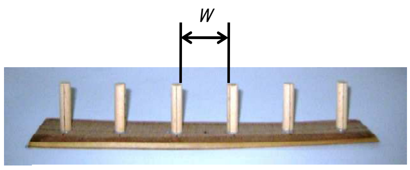

Figure 6: Slit dam model

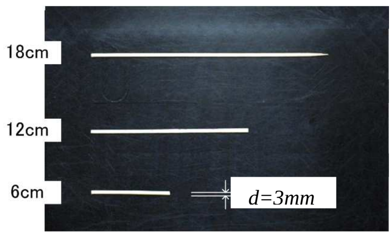

Figure 7: Wooden debris model (*d=3mm*)

2.2 Test conditions

The Froude similarity scale law was applied to this test with the scale factor of 1/50. The test cases are shown in Table 1. Test series I is to examine the effect of the maximum length of wooden debris and the gap of a slit dam on the trap performance. Test series II is to investigate the effects of flow volume and channel slope on the trap performance. Test series III is to examine the effects of average length and the gap of a slit dam on the trap performance.

2.3 Slit dam model

A slit dam model with scale factor of 1/50 for trapping of wooden debris was made by wooden columns with a diameter (d) of 10mm and a height of 4cm as shown in Fig.6. The gap ratio (W/l_{max}) of the slit dam was changed by the test case as shown in Table 1.

2.4 Wooden debris model

Three kinds of wooden debris model were made with lengths of 6cm,12cm,18cm as shown in Fig.7 and two kinds with diameters of 3mm and 6mm. Therefore in total, there were six kinds of wooden debris models in which the specific gravity was 0.8-0.95 for the test.

Table 1: Test case

Series	Gap ratio W/l_{max}	Max.length l_{max} (cm)	Average length l_{mean} (cm)	Diameter d (mm)	Flow volume Q (ℓ/s)	Slope θ (°)	No. of cases
I	1/5 1/3 1/2 3/4	(a)18 (b)12 (c)6	Same as max.length	(i) 6 (ii)3	2.7	3	28
	4/5	(d)18 (e)12					
II	1/2	12	Same as max.length	3	5.6 2.7	5 3 1	6
III	1/5 1/4 1/3 1/2	18	12 10 8	6 3	2.7	3	24

2.5 Test Results

2.5.1 The effect of gap ratio (W/l_{max}) on trap performance (Series I)

Figure 8 shows the effect of gap ratio (W/l_{max}) on the trap performance in the case of the maximum length (l_{max}) of 12cm and the diameter (d) of 3mm. It was found that the number of trapped wooden debris decreases as the gap ratio (W/l_{max}) increases.

Figures 9 (a) and (b) illustrate the effect of gap ratio (W/l_{max}) on the trap ratio in cases of diameters of 3mm and 6mm, respectively. It was confirmed that the trap ratio generally decreases as the gap ratio increases, although the trap ratio with a diameter of 6mm is a little larger than the one of 3mm.

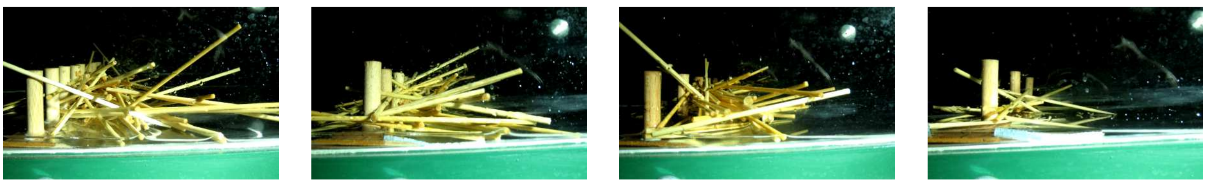

(a) W/lmax=1/5 (b) W/lmax=1/3 (c) W/lmax=1/2 (d) W/lmax=3/4

Figure 8: The effect of gap ratio (W/l_{max}) on trap performance
(Series I-(b)-(ii): l_{max} = 12cm and d = 3mm)

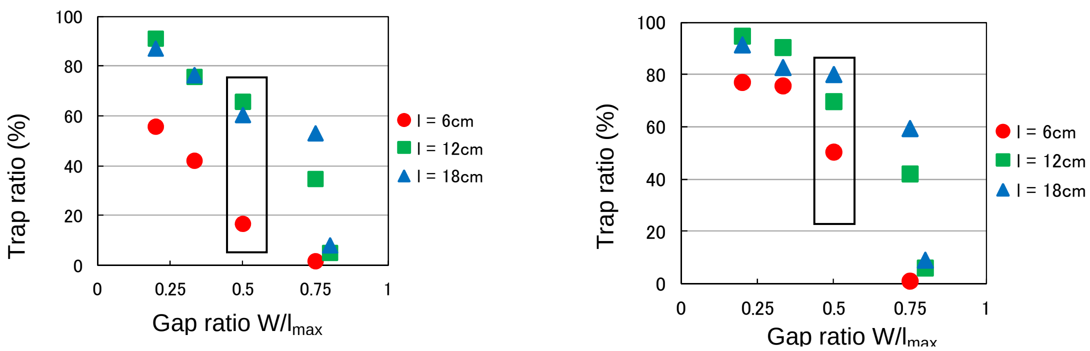

(a) d= 3mm (b) d= 6mm

Figure 9: The effect of gap ratio on the tarp ratio (Series I)

2.5.2 The effect of flow volume *Q* (ℓ/s) on trap performance (Series II)

Figures 10 and 11 show trap processes in cases of flow volume *Q* =2.7ℓ/s and Q=5.6ℓ/s, respectively, at a channel slope $\theta = 3^{\circ}$. In these figures, t_0 represents the arrival time of the 1st wooden debris.

In the case of *Q* =2.7ℓ/s as shown in Fig.10, once a little wooden debris was trapped by the slit dam, successive wooden debris were captured due to the smaller flow volume. However, in the case of *Q* =5.6ℓ/s as shown in Fig.11, it was observed that amassed wooden debris crumbled due to the fluctuation of water's surface, and the scattered wooden fragments overflowed and slipped through the slit dam due to the high flow velocity.

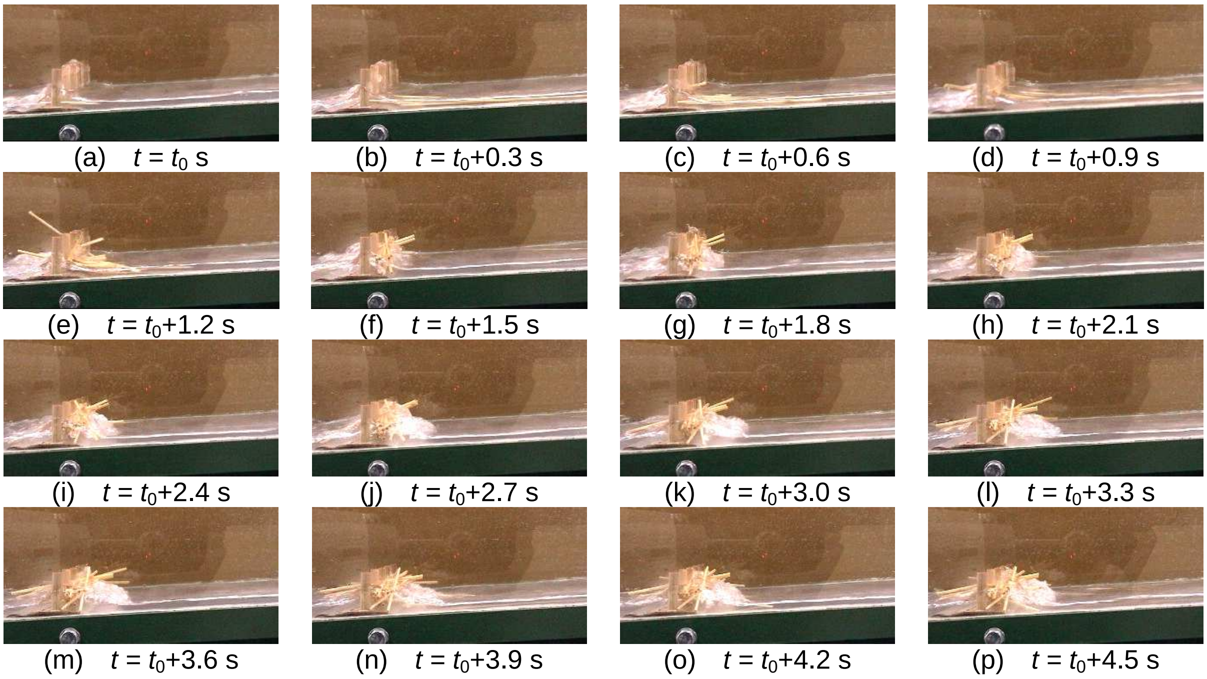

(a) $t = t_0$ s (b) $t = t_0+0.3$ s (c) $t = t_0+0.6$ s (d) $t = t_0+0.9$ s
(e) $t = t_0+1.2$ s (f) $t = t_0+1.5$ s (g) $t = t_0+1.8$ s (h) $t = t_0+2.1$ s
(i) $t = t_0+2.4$ s (j) $t = t_0+2.7$ s (k) $t = t_0+3.0$ s (l) $t = t_0+3.3$ s
(m) $t = t_0+3.6$ s (n) $t = t_0+3.9$ s (o) $t = t_0+4.2$ s (p) $t = t_0+4.5$ s

Figure 10: Trap process of flow volume *Q*=2.7ℓ/s

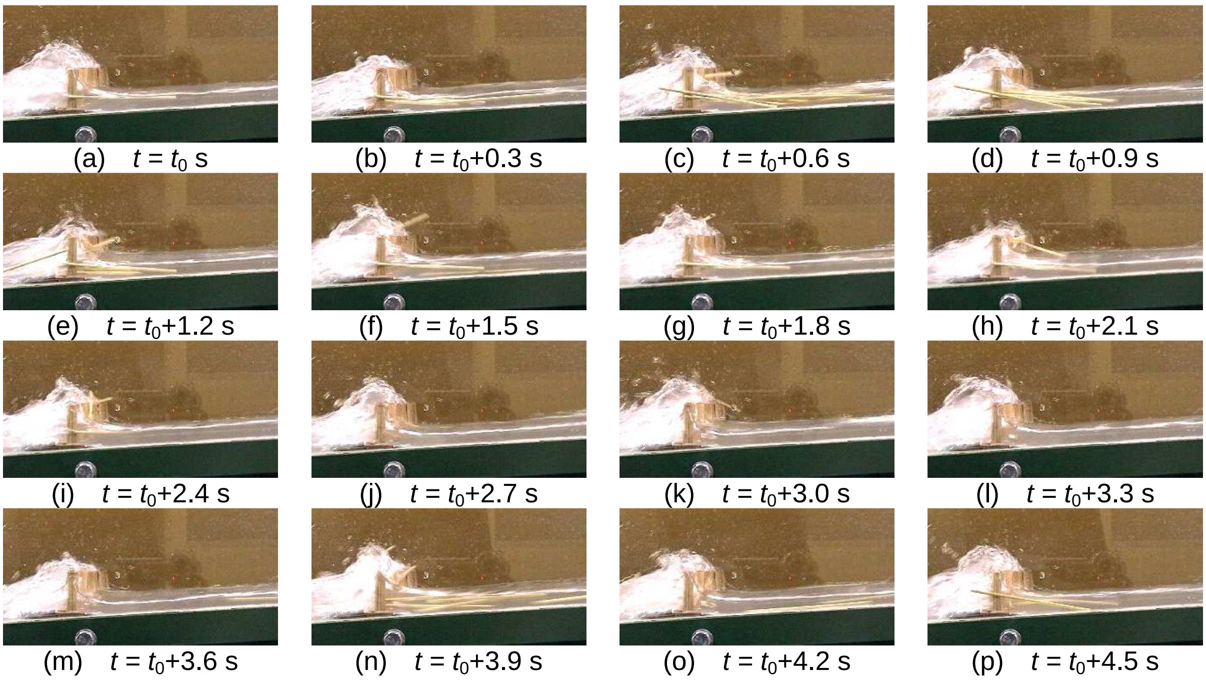

(a) $t = t_0$ s (b) $t = t_0+0.3$ s (c) $t = t_0+0.6$ s (d) $t = t_0+0.9$ s
(e) $t = t_0+1.2$ s (f) $t = t_0+1.5$ s (g) $t = t_0+1.8$ s (h) $t = t_0+2.1$ s
(i) $t = t_0+2.4$ s (j) $t = t_0+2.7$ s (k) $t = t_0+3.0$ s (l) $t = t_0+3.3$ s
(m) $t = t_0+3.6$ s (n) $t = t_0+3.9$ s (o) $t = t_0+4.2$ s (p) $t = t_0+4.5$ s

Figure 11: Trap process of flow volume *Q*=5.6ℓ/s

Figure 12 shows the effect of the flow volume *Q* (ℓ/s) on the final trap performance at the channel slope ($(\theta = 3^{\circ})$). It was found that the trap performance of the smaller flow volume (*Q* =2.7ℓ/s) was better than the one of the larger one (*Q* =5.6ℓ/s), because the fluctuation of water's surface occurred due to the larger flow volume (*Q* =5.6ℓ/s) and, as such, scattered wooden fragments overflowed and slipped through a slit dam as mentioned above.

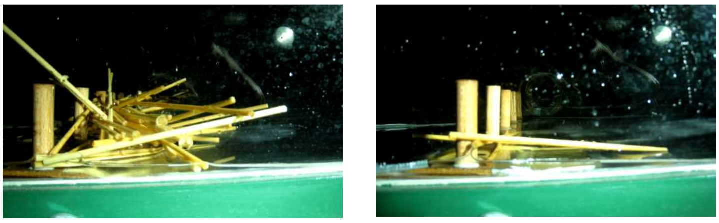

(a) Q =2.7 ℓ/s (b) Q =5.6 ℓ/s

Figure 12: The effect of flow volume *Q* (ℓ/s) on trap performance

2.5.3 The effect of channel slope(θ) on trap ratio (Series II)

Figure 13 illustrates the effect of the channel slope(θ) on the trap ratio by changing flow volume as a parameter. It was confirmed that the trap ratio decreases as the channel slope(θ) increases and the flow volume(*Q*) increases. This is because the flow velocity increases and, therefore, the amassed wooden wreckage was untangled, overflowed or slipped through the slit dam.

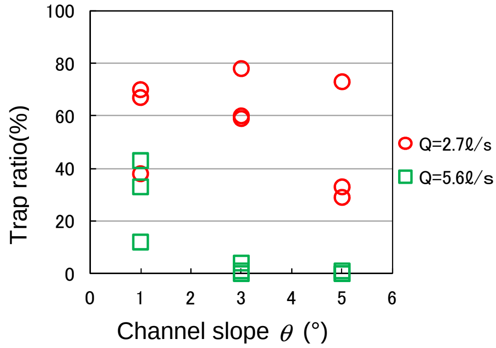

Figure13: The effect of channel slope (θ) on trap ratio

2.5.4 The effect of average length on trap performance (Series III)

Figure 14 shows the effect of average length on the trap performance, in the case of the average length of 10cm ((18cm×10 +12cm×47 +6cm×43)/ 100=10cm). It was found that the trap performance of average length became worse than the one of constant length (Fig.8) with the increase of gap ratio. This is because short sticks, 6cm in average length, were not captured by a slit dam.

(a) W/l_{max}=1/5 (b) W/l_{max}=1/4 (c) W/l_{max}=1/3 (d) W/l_{max}=1/2

Figure 14: The effect of average length on trap performance
(Series III: average length of 10cm, d=3mm)

2.5.5 The effect of average length on trap ratio (Series III)

Figures15 (a) and (b) represent the effect of average length (l_{mean}) on trap ratio at the diameters of 3mm and 6mm, respectively. In the case of the average length of l_{mean} =8cm ((18cm×10+ 12cm×13 + 6cm×77) /100=8cm), the trap ratio is less than 20% as shown in Fig.15 (a), because of too much short length of wooden debris. While in the cases of the average length of 10cm and 12cm, the trap ratios increase as the increase of average length within the range of gap ratio of W/l_{max}=1/3. The trap ratio with the diameter of 6mm as shown in Fig.15(b) increases rather than the one with the diameter of 3mm as shown in Fig.15 (b). This may be due to the larger volume of wooden debris.

It should be noted that the trap ratios of the gap ratio (W/l_{max}=0.2) with the average length in Figs.15 (a) and (b) are almost the same as the ones of the gap ratio (W/l_{max}=0.5) with the maximum length in Figs.9 (a) and (b), respectively. This means that the average length includes a short length of wooden debris and, as such, the gap ratio should be narrowed in order to obtain the same trap ratio.

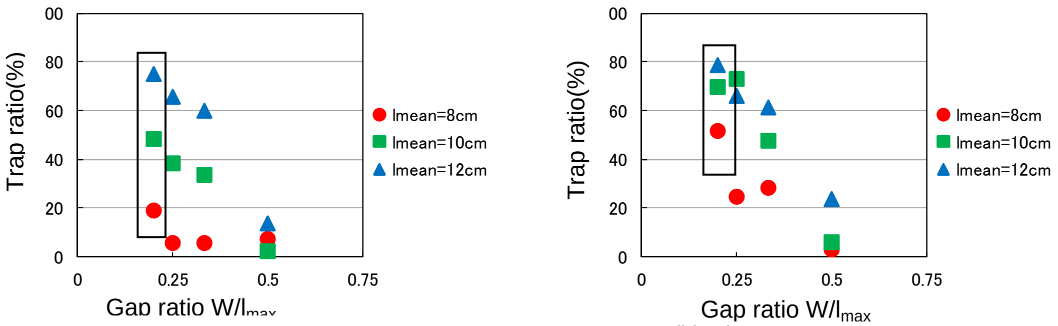

(a) Diameter 3mm (b) Diameter 6mm

Figure15: The effect of average length on trap ratio（Series III）

2.6 Trap mechanism of wooden debris

The trap mechanisms of wooden debris were considered by the test processes of trap formation, as follows.

(1) More than two columns are needed in order to capture a wooden debris.
(2) It is important to make a trigger for the trap in order to catch successive wooden debris.
(3) It is necessary to tangle an amassed wooden debris in order to trap successive wooden debris.

3. COMPUTATIONAL METHOD FOR TRAP PERFORMACE OF WOODEN DEBRIS [15,16]

3.1 A New DEM

A new DEM was developed by introducing the cylindrical stick elements for wooden debris as shown in Figs.16 and 17.

The translation motion is expressed as follows.

$$\mathbf{M}\ddot{\mathbf{u}}(t)+\mathbf{D}\dot{\mathbf{u}}(t)+\sum\mathbf{f}_K(\mathbf{u}(t))=\mathbf{f}_{ex}(t) \quad (1)$$

$$\mathbf{f}_{ex}(t)=\mathbf{M}\mathbf{g}+\mathbf{f}_W(t) \quad (2)$$

where, $\mathbf{M}$: mass matrix, $\mathbf{D}$: damping matrix, $\mathbf{f}_K$: equivalent spring force vector, $\mathbf{u}$: dispalcement vector, $\mathbf{f}_{ex}$: external force vector, $\mathbf{g}$: gravity acceleration vector, $\mathbf{f}_W$: flow force

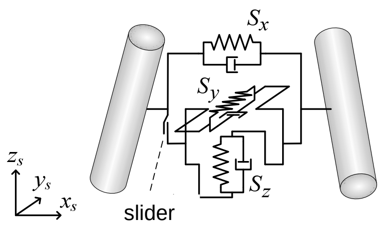

Figure16: Springs between cylindrical stick elements

The equation of rotational motion can be also represented as follows.

$$\left\{\hat{\tilde{\mathbf{I}}}\dot{\hat{\tilde{\boldsymbol{\omega}}}}(t)-\hat{\tilde{\mathbf{P}}}(t)\times\hat{\tilde{\boldsymbol{\omega}}}(t)\right\}+\sum\hat{\tilde{\mathbf{M}}}_D(t)+\sum\hat{\tilde{\mathbf{M}}}_k(t)=\hat{\tilde{\mathbf{M}}}_{ex}(t) \quad (3)$$

$$\hat{\tilde{\mathbf{M}}}_{ex}(t)=\hat{\tilde{\mathbf{M}}}_W(t) \quad (4)$$

where, $\mathbf{I}$: inertia moment matrix, $\boldsymbol{\omega}$: rotational velocity vector, $\mathbf{P}$: rotational momentum vector, $\mathbf{M}_k$, $\mathbf{M}_D$: equivalent moments due to spring and dash-pot, respectively, $\mathbf{M}_{ex}$: external moment vector, $\mathbf{M}_W$: moment due to flow force.

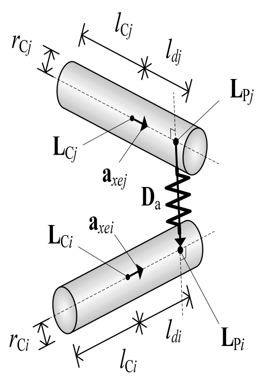

Figure 17: Contact between sides of stick elements

3.2 Flow force due to flow velocity distribution

The flow force is expressed as Eq.(5) by reffering to the flow velocity distribution $\mathbf{U}_{ij}$ ($\mathbf{U}_{ij}^T=[U_{xij}, U_{yij}, U_{zij}]$ as shown in Fig. 18.

$$\mathbf{f}_{\mathrm{W}ij}=\frac{1}{2}C_{\mathrm{D}}\rho w_j A_{ij}\begin{bmatrix}\dot{u}_{\mathrm{Rx}ij}\left|\dot{u}_{\mathrm{Rx}ij}\right|\\ \dot{u}_{\mathrm{Ry}ij}\left|\dot{u}_{\mathrm{Ry}ij}\right|\\ \dot{u}_{\mathrm{Rz}ij}\left|\dot{u}_{\mathrm{Rz}ij}\right|\end{bmatrix}+\mathbf{f}_{\mathrm{B}ij} \qquad (5)$$

where, C_{D} : drag coefficient, ρ : density of water, w_j : weight of integral point j, A_{ij} : projection area to flow direction of element i at integral point j, $\dot{u}_{\mathrm{Rx}ij}$, $\dot{u}_{\mathrm{Ry}ij}$, $\dot{u}_{\mathrm{Rz}ij}$: relative velocity vectors of x, y, z axis of element i at integral point j, $\mathbf{f}_{\mathrm{B}ij}$: buonyancy vector of element i at integral point j.

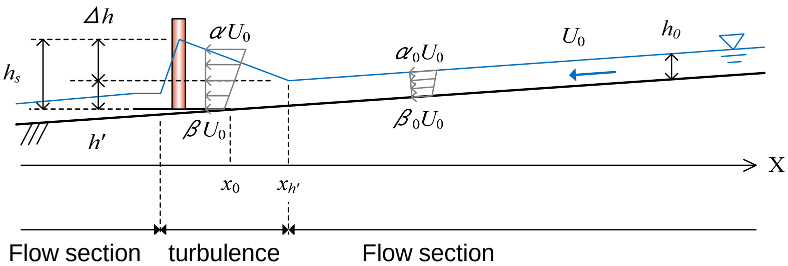

Figure 18: Flow velocity distribution

The effect of fluctuation on the water's surface was introduced as a probabilistic variable based on the normal distribution of vertical flow velocity [15,16] .

3.3 Computational resutls

3.3.1 Input data

The input data was adopted as shown in Table 2. The spring constant of normal direction K_{n} was determined by the compressive test of wooden debris and the one of tangential direction K_{s} was obtained by using the propagation velocity of elastic wave as follows.

$$\frac{K_s}{K_n}=\frac{G}{\lambda+2G}=\frac{1-2\nu}{2(1-\nu)} \qquad (6)$$

where, G, λ : constants of Lame, ν *(=0.4 for cedar)*: Poisson's ratio.

Table 2: Input Data

Item			value
channel	Slope θ		3 °
	Length		3 m
	Width		0.3 m
Flow	Intial velocity U_0		0.8 m/s
	Initial depth h_0		8 mm
	Drag coefficient C_{D}		1.0
Wooden element	Number of element		100
	Density ρ		950 kg/m^3
Spring	Spring constant	Normal direction K_{n}	1.0×10^{6} N/m
		Tangential direction K_{s}	1.5×10^{5} N/m
	Damping constant h		0.2
	Cohesive coefficient c		0 N
	Friction coeffient $\tan\varphi$		0.404
Computation condition	Time increment Δt		1.0×10^{-7} s

3.3.2 Flow process

Figure 19 shows the comparison between test and computation of flow process of wooden debris in the cases of l_{max}=6cm and W/l_{max}=1/2 from the arrival time (t_0s) of the first wooden debris to the time of 5.0s. It was found that the computational results were the same as the test results. Particulaly, some wooden debris slipped through the slit dam at the time of $t = t_0 + 1.0$ s as shown in Fig.19 (b) and trapped at the time of $t = t_0 + 2.0$ s as shown in Fig.19(c). An amassed wooden debris was trapped from the time of $t = t_0 + 3.0$ s to the time of $t = t_0 + 5.0$ s, as shown in Fig.19(d)-(f).

3.3.3 The effect of gap ratio on trap ratio

Figure 20 represents the computational results of relationship between the trap ratio and the gap ratio of slit dam in the case of d=3mm. It was recognized that the trap ratio decreases as the gap ratio increases. This quantitative tendency was also coincided with the test results as shown in Fig.9(a). In particular, the trap rario of l_{max} =6cm fairly decreases as the gap ratio increases. While the trap ratios of l_{max} =12cm and 18cm were larger than 50% within W/l_{max}=3/4 and these results were almost the same as the test results, as shown in Fig.9 (a).

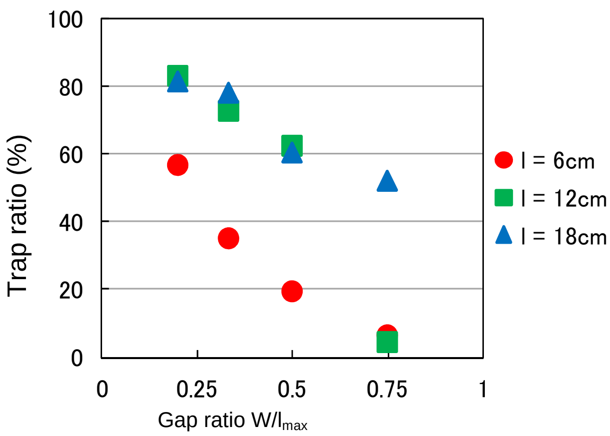

Figure 20: Computational results: The effect of gap ratio on trap ratio (d=3mm)

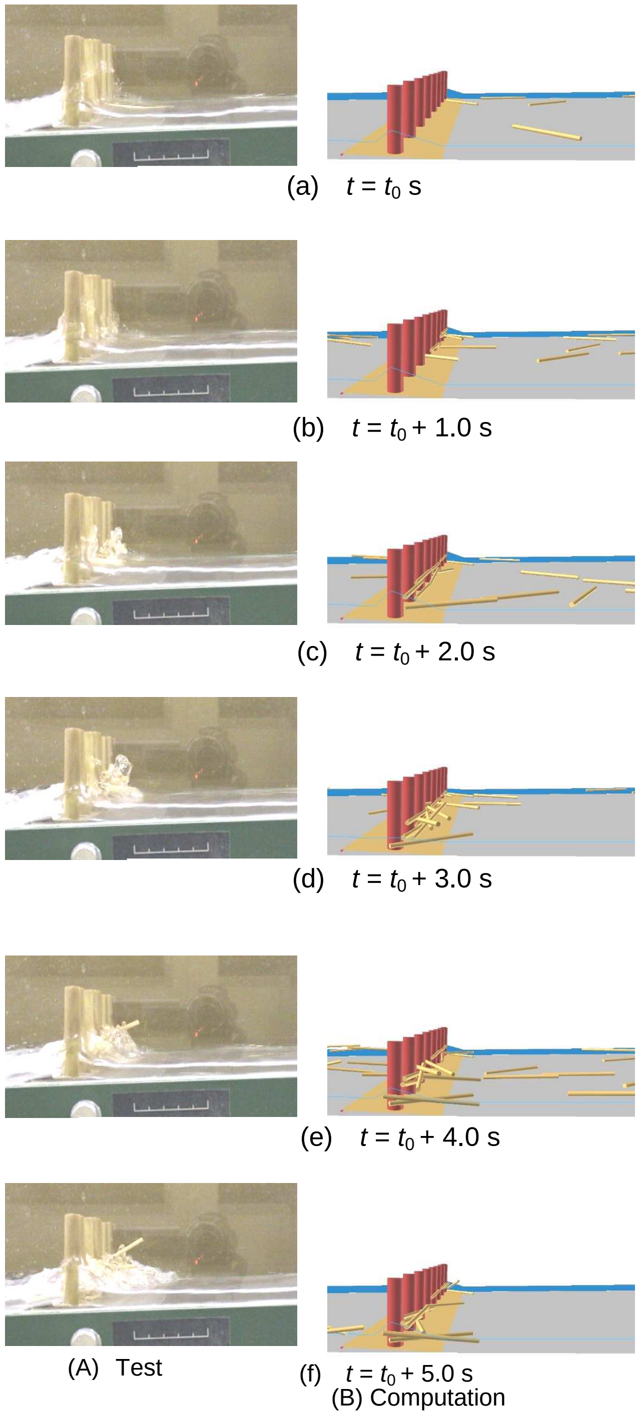

Figure 19: Trap process of wooden debris (l_{max} =6cm, W/l_{max}=1/2)

3.3.4 Comparison between test and computation for trap performance

Figure 21 illustrates the comparison between test and computation for trap performance in the cases of l_{max}=6cm and W/l_{max}=1/5, 1/3, 1/2, 3/4. It was also confirmed that the computational results of W/l_{max}=1/2 and 3/4 did not catch all wooden debris in a similar way to the test resluts, as shown in Fig.21(c) and (d). The computational results at W/l_{max}=1/5 and 1/3, as shown in Fig.21 (a) and (b) captured an amassed wooden debris and this tendency showed matched the test results.

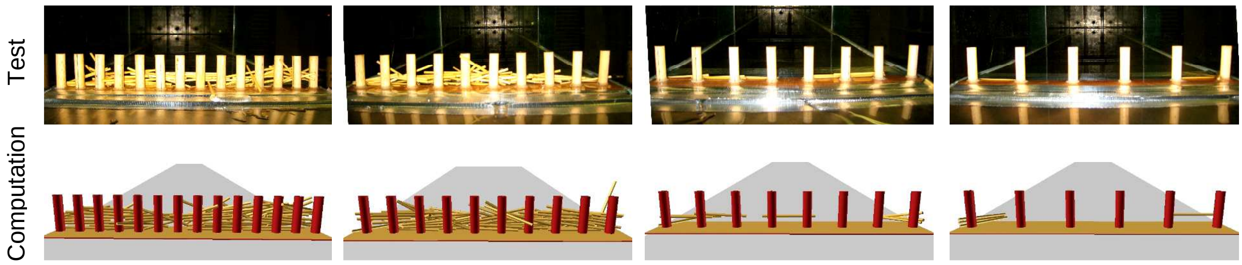

(a) W/l_{max}=1/5 (b) W/l_{max} = 1/3 (c) W/l_{max}= 1/2 (d) W/l_{max}= 3/4

Figure 21: Comparison between test and computation of trap performance (l_{max}=6cm)

3.3.5 The effect of wooden debris with roots

In order to examine the effect of wooden debris with roots, a model test was also conducted by using the specimen as shown in Fig.22(a) and a computation was also performed by using models as shown in Fig.22(b). Nine tests and computations were executed as shown in Table 3.

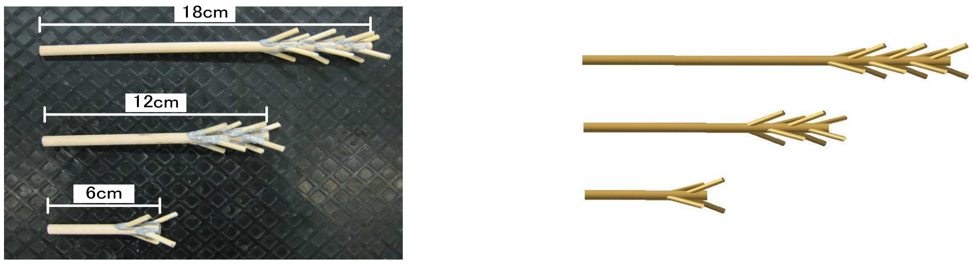

(a) Test model (b) Computation model

Figure 22: Wooden debris model with roots

Table 3: Cases of wooden debris with roots

Trap ratio (W/l_{max})	Length l (cm)	Case
1/3	6	
1/2	12	9
3/4	18	

(1) Comparison between test and computation on trap process by wooden debris with roots

Figure 23 shows the comparison between test and computation of trap performance using wooden debris with roots. The time t_0 means the arrival time of the first wooden debris. First, the blockage of the slit dam was occurred due to the scattered wooden fragments, as shown in Figs.23(a) and (b) and then, the level of amassed wooden debris became higher with a rising of the water level, as shown in Figs.23(c) and (d). Successive wooden debris sedimented in the upper stream,as shown in Figs.23(e)-(f). This computational tendency showed the same result as the test.

(2) Comparison between test and computation on trap performance of wooden debris with roots

Figure 24 illustrates the effect of roots of wooden debris on trap performance. It was obvious that the trap performance of the gap ratio of W/l_{max}=3/4 as shown in Fig.24(c) was better than the case of wooden debris without roots, as shown in Fig.21(d). This is due to the roots, which can easily tangle with columns. The computational results almost coincided with the test.

(3) Comparison between test and computation on trap ratio of wooden debris with roots

Figure 25 represents the effect of gap ratio on trap ratio, comparing the test with the computation of wooden debris with roots. It was apparent that the trap ratios of wooden debris with roots increase rather than the ones without roots, as shown in Fig.9 and Fig.20. It should be noted that the computational results mirror the test results.

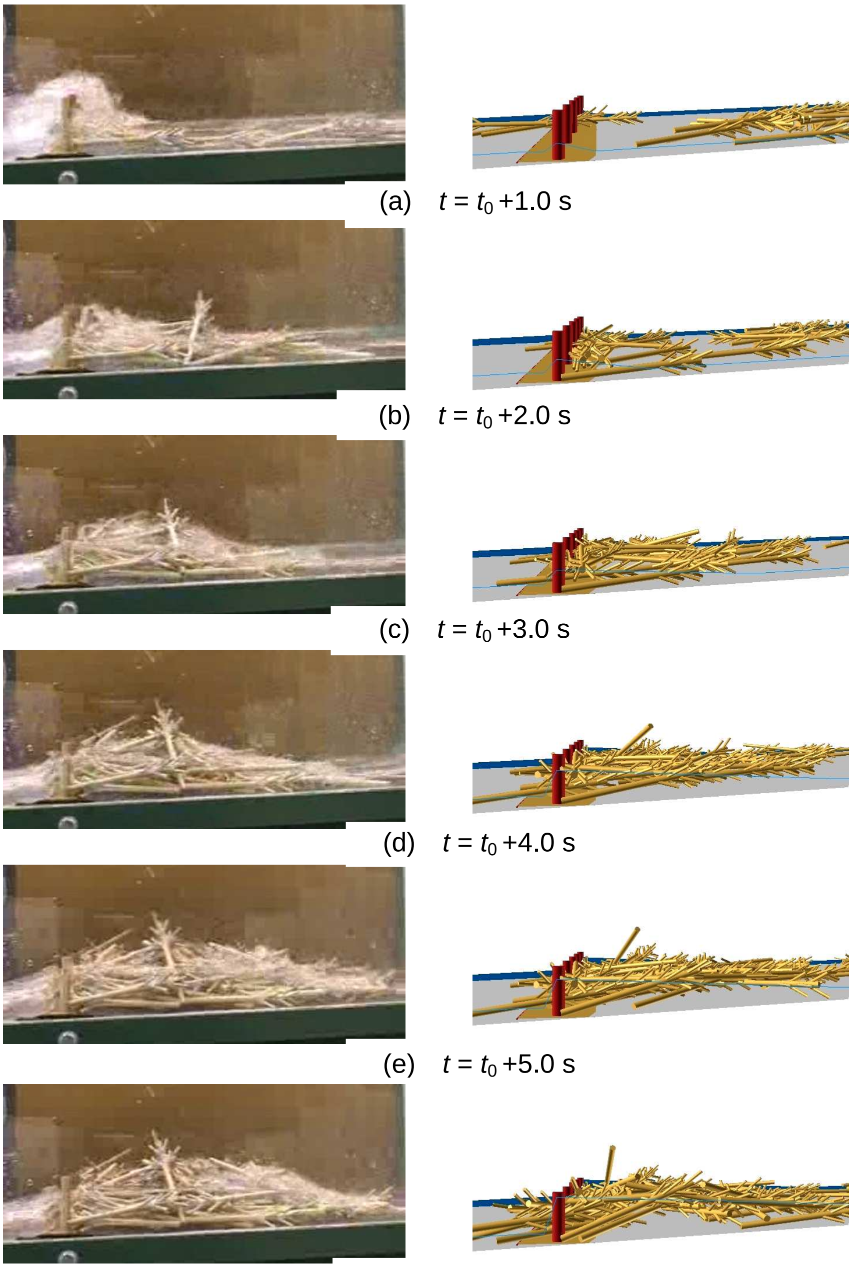

(a) $t = t_0 +1.0$ s

(b) $t = t_0 +2.0$ s

(c) $t = t_0 +3.0$ s

(d) $t = t_0 +4.0$ s

(e) $t = t_0 +5.0$ s

(f) $t = t_0 +6.0$ s

(A)Test (B) Computation

Figure 23: Trap process of wooden debris with roots

(a) W/l_{max}=1/3 (b) W/l_{max}=1/2 (c) W/l_{max}=3/4

Figure 24: Comparison between test and computation of wooden debris with roots (l_{max}=6cm)

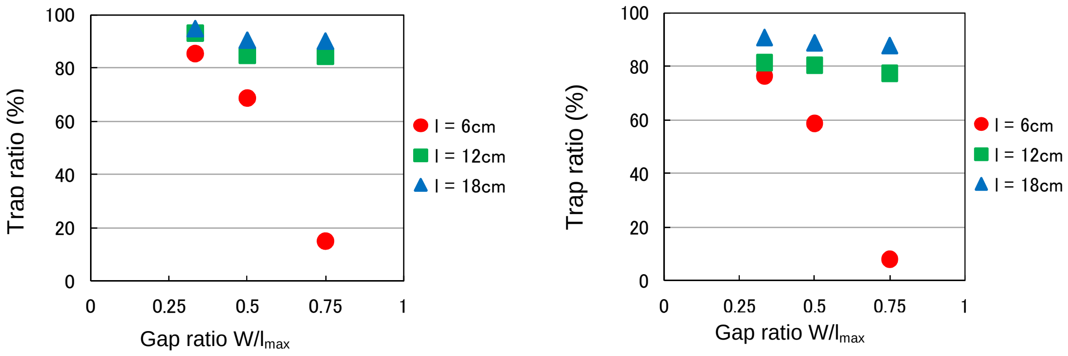

(b) Test (b) Computation

Figure 25: The effect of gap ratio on trap ratio in case of wooden debris with roots

4. APPLICATION TO AN ACTUAL BROCKAGE DISASTER CAUSED BY WOODEN DEBRIS

The brockage of this bridge by scatterd wooden fragments occurred due to a local downpour in Shobara city,Hiroshima, Japan on 16 July 2010 as shown in Fig.24 [18].

The rain which fell on 15 and 16 July were 259mm and 125mm,respectvely, and, as such, the total flow volume was computed as Q_p = 110.8 m^3/s. It was considered that amassed of wooden debris blocked the Bridge B through the Bridge A, as shown in Fig.27. In order to simulate such a brockage disaster, the new developed DEM was applied to simulate the blockage of bridge by using the scenario in Fig.27 and the input data as depicted in Table 4 .

Figure 26: Wooden debris disater

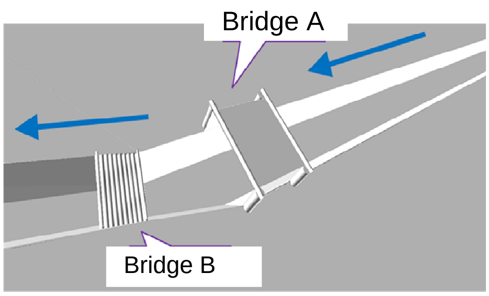

Figure 27: Situation of two bridges

Table 4: Input data for actual wooden debris disaster

Item			value
Flow water	Coefficient of roughness n		0.04 $m^{1/3}/s$
	Drag coefficient C_D		1.0
Element of wooden debris	No. of element		500
	Average length l_{mean}		6.1 m
	Average diameter d_{mean}		25.1 cm
	Density ρ		950 kg/m^3
Spring between elements	Spring constant	Normal direction K_n	1.0×10^7 N/m
		Tangential direction K_s	1.5×10^6 N/m
	Damping coefficient h		0.2
	Cohesion c		0 N
	Friction $\tan\varphi$		0.404
Computing condition	Time increment Δt		2.0×10^{-5} s

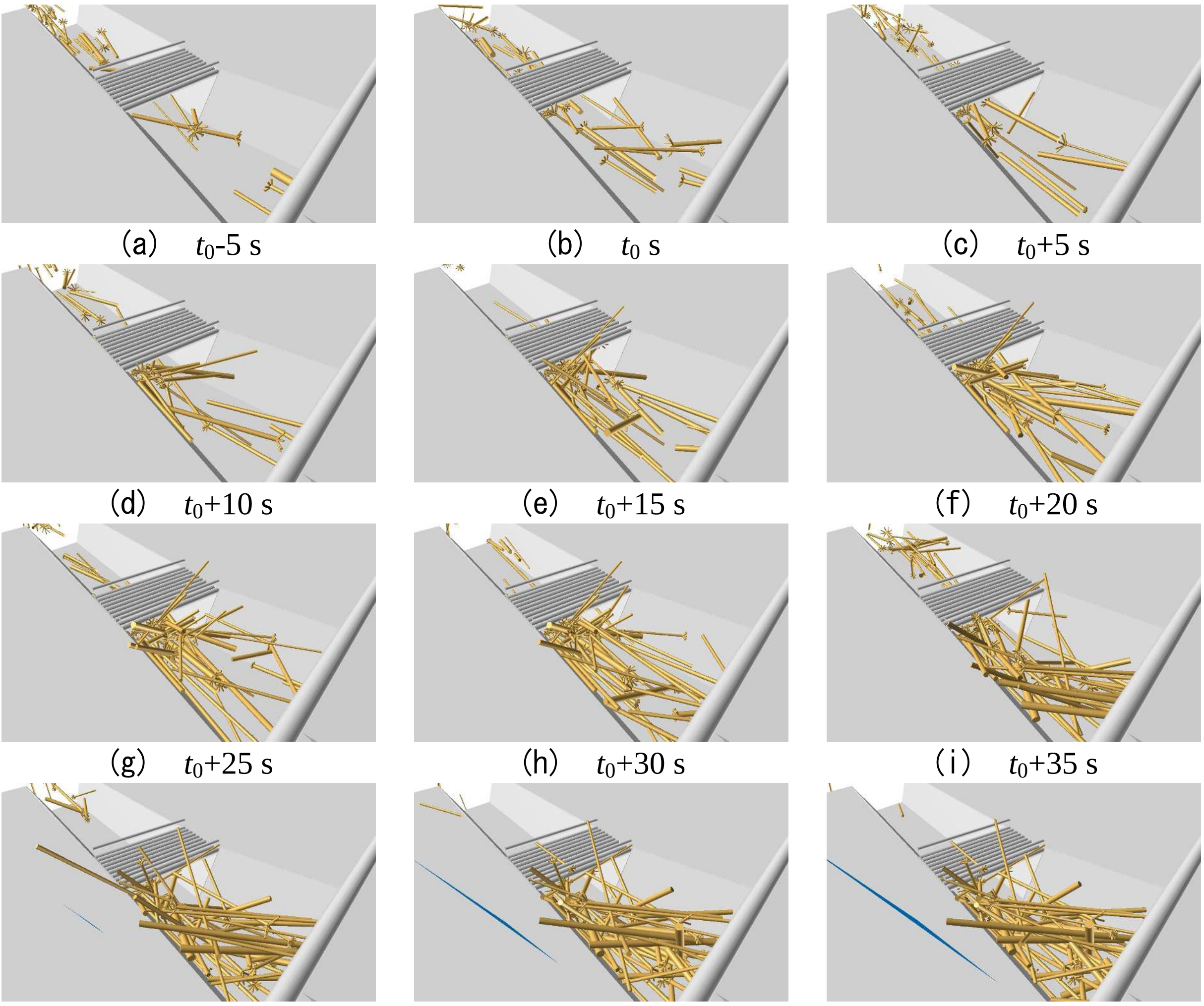

(a) t_0-5 s (b) t_0 s (c) t_0+5 s
(d) t_0+10 s (e) t_0+15 s (f) t_0+20 s
(g) t_0+25 s (h) t_0+30 s (i) t_0+35 s
(j) t_0+40 s (k) t_0+45 s (l) t_0+50 s

Figure 28: Bridge blockage simulation against actual wooden debris

	(a) From down stream	(b) From up stream
Actual disaster		
Computation	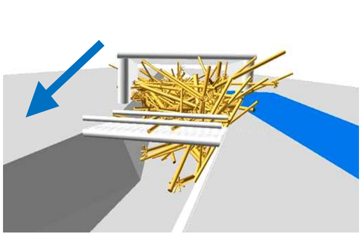	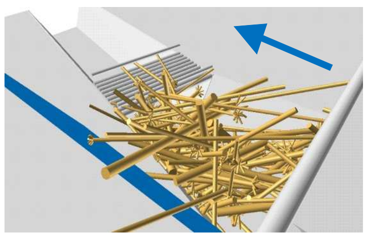

Figure 29: Bridge brockage disaster by wooden debris

Figure 28 shows the computational results of bridge blockage simulation against actual wooden debris by using the new DEM. It was found that an amassed debris flow was trapped by Bridge B from the time of t_0+15 s to the time of t_0+40 s and no outflow of wooden debris occrred from the time t_0+45 s to the time of t_0+50 s.

The final trapping states of the computarion were obtained (a) from the down stream and (b) from the up stream as shown in Fig.29 which compares with the actual disaster. It was recoginized that the final states of trapped wooden debris in the computation were similar to the actual disaster.

If the two columns are placed in front the Bridge A, then an amassed wooden debris would be trapped, as illustrated in Fig.30.

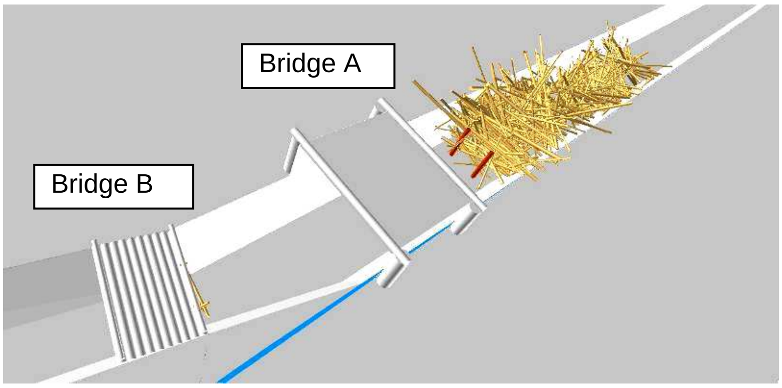

Figure 30: Scenario if the trap columns are placed in front of the Bridge A (flow volume Q=110m^3/s)

5. CONCLUSIONS

The following conclusions were drawn from this study.

(1) It was confirmed that the trap ratio of wooden debris decreases as the gap ratio of the slit dam increases by performing the model test.

(2) It was found that the trap performance of a smaller flow volume of Q =2.7ℓ/s was better than the one of a larger flow volume of Q =5.6ℓ/s, becuase a fluctuation of water's sarface occurred and made the wooden fragments overfow or slip through the slit dam due to the larger flow volume.

(3) It was understood that the trap ratio decreases as the channel slope(θ) increases, because the flow velocity increased, therefore, the amassed wooden wreckage disentangled and overflowed or slipped through the slit dam.

(4) It was recognized that the trap ratio of gap ratio (W/l_{max}=1/5) using the average length was almost the same as the one of the gap ratio (W/l_{max}=1/2) using the constant length.

(5) A new DEM was developed by introducing the cylindrical stick elements for wooden debris and the new DEM could accurately simulate the trap performance of the model tests.

(6) The effect of wooden debris with roots was examined on the trap ratio, which increased, in contrast to the wooden debris without roots. This was obtained from the tests and the computation.

(7) The new DEM was applied to simulate an actual blockage disaster by wooden debris in Hiroshima. The simulation matched the actual disaster rather well.

(8) If the trap columns are placed in front of Bridge A, it would be expected to protect the bridge blockage by using the new proposed DEM.

ACKNOWLEDGEMENTS

The authors are very grateful to the local government staff in Hiroshima for their help in site investigation of the actual wooden debris disaster.

REFERERENCES

[1] Sabo & Landslide Technical Center, Actual conditions of landslide disaster in 2000, p.22,May (2011).
[2] JSCE, Investigation Report on Hokuriku Heavy Rainfall in July 2004, pp.206-220, (2005).
[3] Y.Ishikawa, T.Mizuyama and H.Suzuki, Actual condition and investigation method of wooden debris with debris flow, *Civil Engineering Journal,* Public Works Research Center, Vol.31, No.1, pp.23-29, (1989).
[4] T.Mizuyama, Y.Ishikawa and M.Fukuzawa, Study on movement・sedimentation and countermeasure of wooden debris, *Public Works Research Institution*,Vol.183, No.3, pp.71-156, March (1991).
[5] National Institution for Land and Infrastructure Management, Manual of Technical Standard for establishing Sabo master plan for debris flow and driftwood, *Technical Note*, No.364, Ministry of Land, Infrastructure and Transport, Japan, March (2007).
[6] National Institution for Land and Infrastructure Management, Manual of Technical Standard for designing Sabo facilities against debris flow and driftwood, *Technical Note,* No.365, Ministry of Land, Infrastructure and Transport, Japan, March (2007).
[7] T.Mizuyama, Y.Ishikawa and S.Yajima, Effect of steel slit dams on trap performance of wooden debris, *Civil Engineering Journa*l, Public Work Research Center, Vol.30, No.11, pp.47-52,(1988).
[8] Steel Sabo Structure Committee edited., Design Manual of Steel Sabo Structures, *Sabo & Landslide Technical Center*, (2009).
[9] K.Mizuhara, Sabo dam and wooden debris(I), *Journal of the Japan Society of Erosion Control Engineering*, Vo.28,No.2, pp.17-24, Nov. (1975).
[10] K.Mizuhara, Sabo dam and wooden debris(II), Journal of the Japan Society of Erosion Control Engineering, Vo.28,No.3, pp.17-23, Feb. (1976).
[11] Y.Hasegawa,N.Sugiura, H.Abe, N.Oda, T.Mizuyama and K.Miyamoto, Experimental study on the debris flow including wooden debris, *The Proc. of 2006th Sabo annual meeting* , pp.412-413, (2006).
[12] H.Shibuya, S.Katsuki, N.Ishikawa, H.Ohsumi, Experimental study on trap performance of drift wood capturing structure, *Proceedings of 2nd Specialty Conference on Disaster Mitigation*, CD-ROM 4pages, Winnipeg, Manitoba, Canada, June (2010).
[13] H.Shibuya, S.Katsuki, H.Ohsumi, N.Ishikawa,T,Mizuyama, Experimental study on woody debris trap performance of drift wood capturing structure, *Journal of the Japan Society of Erosion Control Engineering*, Vo.63,No.3 pp.34-41, September (2010).
[14] H.Shibuya, S.Katsuki, H.Ohsumi, N.Ishikawa, Experimental study on trap performance of wooden debris with roots, *Journal of Structural Engineering,* JSCE, Vol.57A, pp.1087-1094,March (2011).
[15] H.Shibuya, S.Katsuki, H.Ohsumi, N.Ishikawa, T,Mizuyama, Analytical study on trap performance of wooden debris by DEM using a cylindrical element, *Proc. of JSCE A2(Applied Mechanics)* , Vo.67,No.1, pp.113-132, October (2011).
[16] S.Katsuki, H.Shibuya: The Distinct Element Method Simulation of Trap Performance of Check Dams used for Wood Contained Debris Flow, *Proceedings of The Tenth International Conference on Computational Structures Technology*, CD-ROM 20pages, Valencia, Spain, September (2010).
[17] Cundall, P. A.: A computer model for simulating progressive, large scale movement in blocky rock system, *Proceedings of the Symposium of the International Society of Rock Mechanics,* Nancy, France, Vol.2, pp.129-136, (1971).
[18] H.Shibuya, S.Katsuki, H.Ohsumi, H.Kokuryo, Investigation of drift wood caused by heavy rain at Shobara, Hiroshima on July 16, 2010, *Journal of the Japan Society of Erosion Control Engineering*, Vo.64,No.1 pp.34-39, May (2011).